ENGINEERING TRANSACTIONS • *Engng. Trans.* • **60**, 1, 15–29, 2012
Polish Academy of Sciences • Institute of Fundamental Technological Research (IPPT PAN)
National Engineering School of Metz (ENIM)
SIXTY YEARS OF THE ENGINEERING TRANSACTIONS

Perforation Modes of Metal Plates Struck by a Blunt Rigid Projectile

Chen XIAOWEI[1)], Liang GUANJUN[2)]

[1)] *China Academy of Engineering Physics*
Institute of Structural Mechanics
P.O.Box 919-401, Mianyang, Sichuan, 621900
e-mail: chenxiaoweintu@yahoo.com

[2)] *Southwest University of Science & Technology*
School of Civil Engineering
Mianyang, Sichuan, 621010

The present paper analyzes the possible modes of shear plugging and adiabatic shear plugging in the perforation of metal plates struck by a blunt rigid projectile. The modified ballistic limit and residual velocity under the condition of adiabatic shear plugging are further formulated. Further experimental analyses are conducted on the perforations of Weldox E steel plates in order to discuss the effects of plate thickness and material strength/hardness on the terminal ballistic performance. More experimental evidence confirms the jump of residual velocity at the ballistic limit induced by the structural response of the plate. With increasing the thickness of plate and the material strength, failure modes of the plate may transform from shear plugging to adiabatic shear plugging.

Key words: blunt rigid projectile, metallic plate, perforation, shear plugging, adiabatic shear plugging.

1. Introduction

Perforation of intermediate thick metallic plates by a blunt rigid projectile has been paid much attention [1–7] for a long time because of its civil and military applications, and recent work may be referenced to Børvik *et al.* [2, 8–11], Dey *et al.* [4], Chen and Li [12–13], and Chen *et al.* [1, 14–16]. With increasing the plate thickness and impact velocity, shear plugging becomes a likely failure mode of the final perforation of an intermediate thick metallic plate.

There exist many analytical models to predict the ballistic performance, e.g. Wen and Jone [17], Bai and Johnson [18], and Ravid and Bodner [19].

Based on the conservation of momentum and energy, Recht and Ipson [20] proposed a shear plugging model to predict the residual velocity according to a given impact velocity and a ballistic limit velocity obtained from a dimensional analysis. Recht and Ipson [20] completely ignore the structural response for relatively thin plates and the local penetration for relatively thick plate. Using the energy-balance approach, Srivathsa and Ramakrishnan [21, 22] derived a ballistic performance index to estimate and compare the ballistic quality of metal materials. This index is a function of the commonly determined mechanical properties of the target material and the striking velocity of the projectile. Chen and Li [12] presented closed-form analytic solutions for ballistic perforation of ductile circular plates struck by blunt projectiles. In addition to the localized shear deformation at the peripheral of the central plug, their rigid-plastic structural model also considered the effect of plate bending and membrane stretching. The local indentation/penetration employs a dynamic cavity model. With the assistance of numerical simulation, Chen *et al.* [16] further discuss the applicability of this model and its discrepancy when compared to the experimental results and simulation.

Basically, the perforation mechanism of the ballistic performances depends on the target material property (e.g., strength or hardness), target dimensions, projectile nose shape, mass and impact velocity. By means of experiment and numerical simulation, Børvik *et al.* [2] and Dey *et al.* [3] systematically analyzed the effect of target thickness and strength on the ballistic performance. In general, the ballistic limit rises monotonically with increasing the target thickness and strength when the shear plugging dominates in the perforation of the plate. However, the perforation is always an adiabatic heat process and under the adiabatic condition, the majority of the plastic energy is converted into heat. This generates localized high temperature and adiabatic shearing occurs when the thermal softening outbalances the incremental strain and the strain-rate hardening of the target material, which eventually leads to the catastrophic failure within the Adiabatic Shear Band (ASB). With increasing the target thickness and strength, the failure mode easily transform from shear plugging to adiabatic shear plugging. ASB distinctly influences the ballistic performance, and one deduction is that the monotonic relationship between the ballistic limit and target thickness and strength never come into existence. Instead, it becomes an approximate relationship [23, 24]. With further considering the possible transforming mechanism of material failure, Chen *et al.* [1] check the initiation condition for adiabatic shear band failure and present the criterion of adiabatic shear plugging in the case of a blunt projectile perforating a metallic plate.

Based on the analytical models by Chen and Li [12] and Chen *et al.* [1], the present paper analyzes the possible modes of shear plugging and adiabatic shear plugging in the perforation of metal plates struck by a blunt rigid projectile. The modified ballistic limit and residual velocity under condition of adiabatic shear plugging are further formulated. Further experimental analyses are conducted on the perforations of Weldox E steel plates [2, 3], to discuss the effects of plate thickness and material strength/hardness on the terminal ballistic performance.

2. Shear plugging and perforation of ductile circulate plates struck by a blunt projectile

Chen and Li [12] studied the formation of shear plug during the perforation of ductile circular plates struck by a blunt projectile. In their studies, the effects of shear, plate bending, and membrane stretching were considered via a rigid-plastic analysis, while the local indentation/penetration was represented in a dynamic cavity expansion model.

Consider a blunt projectile of mass M and caliber d impacting a clamped ductile circular plate of thickness H and diameter D. The yielding stress and density of target material are σ_y and ρ respectively. Thus the dimensionless thickness and mass of target are $\chi = H/d$ and $\eta = \rho\pi d^2 H/4M$ respectively. The intermediate thick plate and plate bending are included only, i.e., membrane stretching and local indentation/penetration are ignored. It corresponds to the case of $\chi_1 < \chi \leq \sqrt{3}\,(A + B\Phi_J)/4$, in which χ_1 is the empirical upper limit of thin plate and it depends on the target material and diameter D, usually we have $\chi_1 \approx 0.2$. A and B are the dimensionless material constants used in the dynamic cavity model.

It is assumed that a central plug will be formed in front of the projectile at a critical condition when the total compressive force on the projectile nose equals to the fully plastic shear force on the peripheral of the plug. After the plug is formed, it moves with the projectile under constant shear resistance, Q_0, which is equal to $H\tau_y = H\sigma_y/\sqrt{3}$ according to the von Mises yielding criterion, where τ_y and σ_y are the shear yield stress and compressive yield stress of the material, respectively. Dimensionless mass between the central plug and projectile is denoted by $\eta = \rho\pi d^2 H/4M$. $M_0 = \sigma_y H^2/4$ and $N_0 = \sigma_y H$ are the fully-plastic bending moment and membrane force in a rigid-perfectly-plastic circular plate, respectively. With considering the plate bending, Chen and Li [12] presents the ballistic limit of plate and residual velocity of projectile are as following,

$$
V_{BL} = 2\sqrt{\frac{2\chi\,(1+\eta)\,(\eta+\vartheta)}{\sqrt{3}}} \cdot \sqrt{\frac{\sigma_y}{\rho}},
\tag{2.1}
$$
$$
V_r = \frac{\vartheta V_i + \eta\sqrt{\left(V_i^2 - V_{BL}^2\right)}}{(1+\eta)\,(\eta+\vartheta)} \geq V_{\mathrm{Jump}}.
$$

Regarding the residual velocity, a jump of residual velocity

$$V_{\mathrm{Jump}} = \frac{\vartheta V_{BL}}{(1+\eta)(\eta+\vartheta)} > 0$$

exists at the ballistic limit. ϑ in Eqs. (2.1) is a dimensionless parameter which depends on the plate thickness and diameter,

$$\vartheta = \begin{cases} \dfrac{3\left(1-\sqrt{3}\chi\right)(1+\eta)}{2\left(2\xi/d-1\right)\left(\xi/d+1\right)}, & \chi_1 < \chi < \dfrac{1}{\sqrt{3}}\left[\dfrac{(D/d)^2-1}{(D/d+1)^2+2}\right], \\ \dfrac{3\left(1-\sqrt{3}\chi\right)(1+\eta)}{(D/d-1)(D/d+2)}, & \dfrac{1}{\sqrt{3}}\left[\dfrac{(D/d)^2-1}{(D/d+1)^2+2}\right] \le \chi < \dfrac{1}{\sqrt{3}}. \end{cases} \tag{2.2}$$

If $1/\sqrt{3} \le \chi \le \sqrt{3}\,(A+B\Phi_J)/4$, we have $\vartheta = 0$, and in that case, Eq. $(2.1)_2$ of residual velocity is same as Recht and Ipson [20]. ξ in Eq. (2.2) denotes the stationary location of a bending hinge during the shear sliding phase, and we have [12],

$$\frac{\xi}{d} = \begin{cases} \dfrac{\sqrt{3}\chi + \sqrt{1+2\sqrt{3}\chi - 6\chi^2}}{2\left(1-\sqrt{3}\chi\right)}, & \chi_1 < \chi < \dfrac{1}{\sqrt{3}}\left[\dfrac{(D/d)^2-1}{(D/d+1)^2+2}\right], \\ \dfrac{D}{2d}, & \dfrac{1}{\sqrt{3}}\left[\dfrac{(D/d)^2-1}{(D/d+1)^2+2}\right] \le \chi < \dfrac{1}{\sqrt{3}}. \end{cases} \tag{2.3}$$

3. Transition Criteria from shear plugging to adiabatic shear plugging

The target material property (e.g., strength or hardness), target thickness and impact velocity have obviously influence on the ballistic performances of a blunt projectile impacting on a metallic plate. Under the adiabatic condition, accompanied with increasing the target thickness and strength, the failure mode easily transforms from shear plugging to adiabatic shear plugging or to the hybrid of these two modes. ASB distinctly influences the ballistic performance, and Chen *et al.* [1] further check the initiation condition for adiabatic shear band failure for the case of a blunt projectile perforating a metallic plate.

The characteristic width of a shear hinge is $e_b = \alpha H/3$, and α is an empirical coefficient,

$$\alpha = \begin{cases} 1, & V_i/c_p < 1; \\ \exp\left[C\left(1 - V_i/c_p\right)\right], & V_i/c_p \ge 1, \end{cases} \tag{3.1}$$

where $c_p = \sqrt{E_h/3\rho}$ is the propagating velocity of shear hinge disturbance and E_h is the linear hardening modulus which may decrease due to thermal softening. C is an empirical constant and suppose $C = 5$. More details on the discussion of the characteristic width of a shear hinge can be found in CHEN *et al.* [1]. Consequently, in case of un-perforation or ballistic limit, i.e., $V_i \leq V_{BL}$, the maximum engineering shear strain and the average shear strain rate within the shear hinges around the peripheral of the striker are calculated respectively as follows [1],

$$\gamma_1 = \frac{3\sqrt{3}}{16\alpha\chi(1+\eta)(\eta+\vartheta)} \cdot \frac{\rho V_i^2}{\sigma_y}, \qquad \dot{\gamma}_1 = \frac{3}{4\alpha(1+\eta)} \cdot \frac{V_i}{H}. \tag{3.2}$$

Whereas in case of perforation, i.e., $V_i > V_{BL}$, the maximum engineering shear strain and the average shear strain rate within the shear hinges are different,

$$\gamma_{1*} = \frac{1.5}{\alpha}, \qquad \dot{\gamma}_{1*} = \frac{2\sqrt{3}(\eta+\vartheta)}{\alpha\left[V_i - \sqrt{\left(V_i^2 - V_{BL}^2\right)}\right]} \cdot \frac{\sigma_y}{\rho d}. \tag{3.3}$$

Taking into account the effects of temperature and strain-rate, and using the Johnson-Cook flow law, we have a simple shear constitutive equation of the following form:

$$\tau = \frac{1}{\sqrt{3}}\left[a + b\left(\frac{\gamma}{\sqrt{3}}\right)^n\right]\left[1 + c\ln\left(\frac{\dot{\gamma}}{\sqrt{3}\dot{\varepsilon}_0}\right)\right]\left[1 - \left(\frac{T - T_r}{T_m - T_r}\right)^m\right] \tag{3.4}$$

in which the von Mises equivalent stress, strain, and strain rate (i.e., $\tau = \sigma/\sqrt{3}$, $\varepsilon = \gamma/\sqrt{3}$ and $\dot{\varepsilon} = \dot{\gamma}/\sqrt{3}$) are used in the formulation. The parameters: a (or $a = \sigma_y$), b (nearly as E_h), c and n are all material constants, and $\dot{\varepsilon}_0$ is a prescribed reference strain rate. T_r and T_m are respectively the environmental reference temperature and the melting temperature of target material.

The adiabatic temperature-rise within the shear hinges may be integrated by the formula $dT = \dfrac{\beta}{\rho\, C_V}\tau\, d\gamma$ and Eq. (3.4). Simply, we have $m = 1$, and C_V is the specific heat and β is the Taylor-Quinney coefficient. Usually, the strain-rate effects are measured by its average value during the dynamic deformation. Thus, the expression for the maximum shear stress ($d\tau = 0$) criterion with constant strain-rate ($d\dot{\gamma} = 0$) is [25],

$$\frac{\partial\tau}{\partial\gamma} + \frac{\beta\tau}{\rho\, C_V} \cdot \frac{\partial\tau}{\partial T} = 0. \tag{3.5}$$

According to the definitions of maximum engineering shear strain and average shear strain rate within the shear hinges, i.e. Eqs. (3.2), (3.3). The critical velocity V_A corresponding to the initiation of adiabatic shear failure may be deducted from Eq. (3.5) [1]. Hence, we have,

$$\begin{gathered}
\left[a+b\cdot\left(\frac{3\rho V_A^2}{16\alpha\chi\left(1+\eta\right)\left(\eta+\vartheta\right)\sigma_y}\right)^n\right]^2\left[1+c\ln\left(\frac{\sqrt{3}V_A}{4\alpha\left(1+\eta\right)\dot{\varepsilon}_0 H}\right)\right] \\
=\frac{nb\rho C_V\left(T_m-T_r\right)}{\beta}\cdot\left(\frac{3\rho V_A^2}{16\alpha\chi\left(1+\eta\right)\left(\eta+\vartheta\right)\sigma_y}\right)^{n-1}, \quad \text{if } V_i\le V_{BL}, \\
\left[a+b\cdot\left(\frac{\sqrt{3}}{2\alpha}\right)^n\right]^2\left[1+c\ln\left(\frac{2\left(\eta+\vartheta\right)}{\alpha\left[V_A-\sqrt{\left(V_A^2-V_{BL}^2\right)}\right]\dot{\varepsilon}_0}\right)\right] \\
=\frac{nb\rho C_V\left(T_m-T_r\right)}{\beta}\cdot\left(\frac{\sqrt{3}}{2\alpha}\right)^{n-1}, \quad \text{if } V_i>V_{BL}.
\end{gathered} \tag{3.6}$$

Actually, Eqs. (3.6) are the explicit relations among the critical velocities corresponding to adiabatic shear failure, target thickness, target parameters (material hardness, density and mechanics etc.) and projectile parameters (geometry, mass).

4. Adiabatic shear plugging of ductile circulate plates struck by a blunt projectile

Once the initiation condition for adiabatic shear band failure is achieved for the case of a blunt projectile perforating a metallic plate, the adiabatic temperature-rise within the shear hinges will cause the material thermal softening in the local zone, and thus the material failure of the target will be reached much more easily, as it requires less energy compared to shear failure. It is reasonable that the failure mode of blunt projectile perforating a metallic plate will transform from shear plugging to adiabatic shear plugging. Therein the perforation includes two possible failure modes, i.e, shear plugging and adiabatic shear plugging. The ballistic performance of the first mode can be completely depicted by Sec. 2. Regarding the second mode, i.e., adiabatic shear plugging, the perforation scenarios are much more complicated and respectively need to be analyzed.

1. $V_A \le V_{BL}$

Adiabatic shear plugging occurs prior to the shear plugging, and it is concluded that the perforation mode is the first one. Thus, the ballistic limit is modified as

$$V_{ASB-BL} = V_A. \tag{4.1}$$

Chen *et al.* [1] indicated that this scenario corresponds to a thicker plate and the structural response of the plate is ignored. Under higher impact velocity than the ballistic limit, the residual velocity of both projectile and plug is

$$V_r = \sqrt{\left(V_i^2 - V_{ASB-BL}^2\right)} \Big/ (1+\eta). \tag{4.2}$$

2. $V_A > V_{BL}$

Chen *et al.* [1] indicated that this scenario corresponds to a thinner plate and the structural response of the plate should be taken into account.

In the case of an un-perforation or in the ballistic limit, i.e., $V_i \le V_{BL} < V_A$, no adiabatic shear plugging occurs.

If $V_{BL} < V_i < V_A$, the projectile perforates the plate as shear plugging and no adiabatic shear failure occurs. Therein its ballistic performance is formulated by Eq. (2.1) of Sec. 2.

If $V_i \ge V_A$, the projectile perforates the plate as adiabatic shear plugging. Since the failure mode is transformed, the residual velocity of Eq. $(2.1)_2$ is modified to

$$V_r = \frac{\vartheta V_i + \eta\sqrt{\left(V_i^2 - V_{ASB-BL}^2\right)}}{(1+\eta)(\eta+\vartheta)} \tag{4.3}$$

and we suppose $V_{ASB-BL} = V_A$ here.

Furthermore, during the transformation from shear plugging to adiabatic shear plugging, the material failure mode in the shear hinge is not absolutely singleness. The experimental results indicate that it should be a hybrid of shear failure and adiabatic shear failure. More generally, we suppose that the ballistic limit of the adiabatic shear plugging has the following relationship,

$$V_{ASB-BL} = (1-\delta)\cdot V_A + \delta \cdot V_{BL}, \qquad \text{where} \quad 0 < \delta \le 1, \tag{4.4}$$

where the value of δ depends on which one dominates in the target material failure. If $\delta = 0.5$, we have $V_{ASB-BL} = (V_A + V_{BL})/2$. Employing Eq. (4.4) into this section, the modified ballistic performance of blunt projectile perforating metallic plate as adiabatic shear plugging is obtained.

5. Experimental analyses

Chen and Li [12] first theoretically explained some special phenomenon, such as, that the residual velocity will behave as a jump near the ballistic limit in the case of perforation of a thin metallic plate and the ballistic limit abnormally descend with increasing the target thickness regarding a range of plate thicknesses. The present paper further analyzes the experimental data of Børvik *et al.* [2] and Dey *et al.* [3] and again confirm these special phenomenon. Also we will discuss the applicability of Chen and Li [12], Chen et al. [1] and the present modified model with changing the target thickness and strength.

The present analytical model assumes that the projectile and plug have the same residual velocity after perforation. In order to compare the analytical results with experimental data, a nominal residual velocity in a test is defined based on the conservation of momentum

$$V_r = \frac{M \cdot V_{pr} + M_{pl} \cdot V_{plr}}{(M + M_{pl})}, \tag{5.1}$$

where, in a test, V_{pr} and V_{plr} are the residual velocities of the projectile and the target plug respectively. The mass of target plug is $M_{pl} = \pi \rho d^2 H/4$.

The target material in Børvik *et al.* [2] is Weldox460E and the corresponding material properties can be found in that reference. Dey *et al.* [3] employed three steel alloys of Weldox460E, Weldox700E and Weldox900E, which have different yielding strength, i.e., 499 MPa, 859 MPa and 992 MPa, respectively. The blunt projectile is made of high strength steel of Arne with $\sigma_y = 1900$ MPa. Its mass is 0.197 kg, and its diameter and length are 20 mm and 80 mm respectively.

5.1. *Effect of target thickness on the ballistic performance*

Børvik *et al.* [2] published a large amount of experimental results on the ballistic performance of ductile plates struck by blunt projectiles, as seen in Fig. 1. Their plate thicknesses ranged from thin to intermediate, i.e., target thickness are $H = 6$ mm, 8 mm, 10 mm, 12 mm, 16 mm, and 20 mm respectively. The corresponding dimensionless thickness are $\chi = 0.3$, 0.4, 0.5, 0.6, 0.8, and 1.0, respectively.

The experimental results of Børvik *et al.* [2] showed that regarding relatively thin plates, i.e., $\chi = 0.3$, 0.4 and 0.5, due to the bending response of plate, a jump of residual velocity occurs at the ballistic limit and its value decreases with raising the target thickness; whereas regarding the thick targets ($\chi = 0.6$, 0.8 and 1.0), the curves of residual velocity vary continuously. Figure 1 demonstrates the comparison between experimental data and theoretical predictions by Chen and Li [12], and it clearly shows validation of Chen and Li's [12] model. The experimental data are the weighted average values of the residual velocities of projectile and plug.

Figure 2 shows the effect of target thickness ($\chi = H/d$) of Weldox 460E on the ballistic limit. The test data of Børvik *et al.* [2] showed that regarding

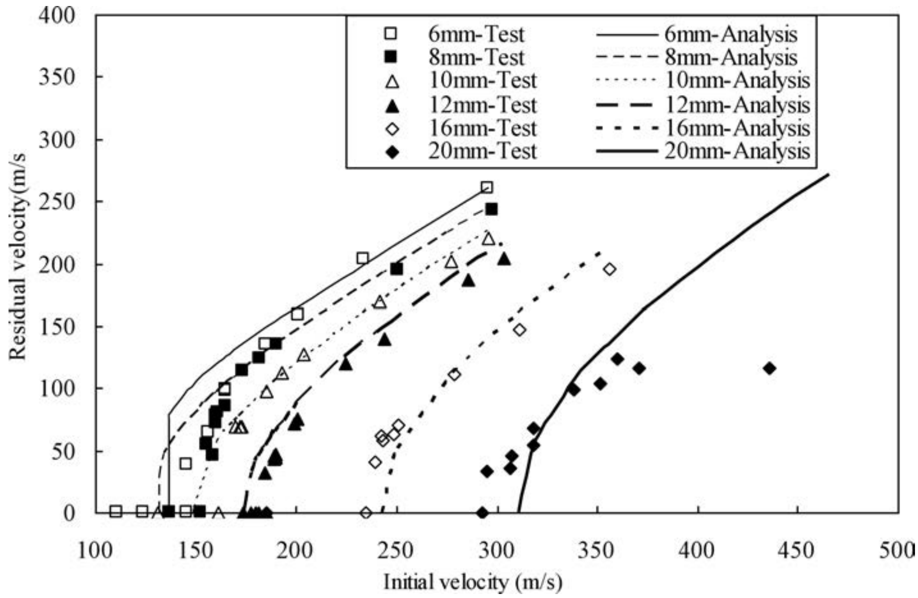

Fig. 1. Comparison between the prediction from Chen and Li [12] and the test data of ballistic performances [2].

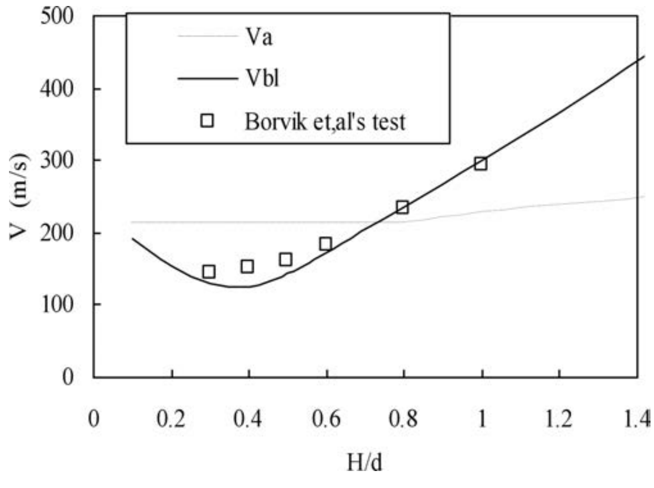

Fig. 2. Variations of critical velocities for the ballistic limit (V_{BL}) and initiation of adiabatic shear (V_A) against plate thickness (H/d).

the thin plates, the ballistic limit rises very slowly with increasing the target thickness; differently, it rises linearly and distinctly regarding the thick plates. Further popularly, Chen and Li [12] indicate in a range of target thickness that it is due to the structural response of thin plate that results in the abnormal descending of ballistic limit with increasing target thickness.

Figure 2 simultaneously presents the prediction of the critical velocity of adiabatic shear failure with varying thickness. Børvik *et al.* [2, 8, 9] also analyzed the different failure modes of the perforation of plates with different thickness. It demonstrates that with increasing the target thickness, the deformation of plate transforms from structural response of thin plate and local shear plugging to adiabatic shear failure. The adiabatic shear failure behaves as a deformed ASB and a transformed ASB respectively.

It is emphasized that the two theoretical curves in Fig. 2 intersect at $\chi = 0.7$. This indicates that, in the case of $\chi < 0.7$, as $V_A > V_{BL}$, even if the impact velocity is greater than the ballistic limit, the target failure may be still shear plugging. The adiabatic shear failure does not easily occur, and it requires a higher impact velocity, i.e., $V_i > V_A$. In case of $\chi > 0.7$, as $V_A < V_{BL}$, adiabatic shear failure may appear easily, even if impact at lower velocity and no perforation. In particular, the ballistic limit should be modified based on Eq. (4.4) because of the hybrid of failure modes. In Fig. 2, the test data locate much close to the prediction of shear plugging, and it indicates the shear plugging dominates in the perforation rather than adiabatic shear failure. Therein suggest $\delta = 0.9$ in Eq. (4.4) regarding Børvik *et al.* [2] test.

Chen *et al.* [1] discussed in detail the variation of adiabatic temperature-rise, strain and strain rate against the target thickness and impact velocity in a local shear zone, which agrees well with the experimental results and numerical simulation. Here, this is not repeated.

Regarding the thin plates, the prediction of the ballistic limit and jump of residual velocity in Fig. 1 is somehow discrepant from the test data. Chen and Li [12] also presented a thinner plate model with considering the membrane effect, and demonstrated that the test data is located between the predictions of thinner and medium plates. However, regarding the thicker plates, e.g., $\chi = 1.0$, the discrepancy of residual velocity between the prediction and test of residual velocity is due to the assumption of rigid projectile. In that case, the projectile deforms and blunts more seriously and much more impact energy is devoted to the plastic deformation of projectile. The projectile even breaks when it perforates much thicker plates, e.g., $\chi = 1.25$ or $\chi = 1.5$. Therein, the model of Chen and Li [12] has its specific applicability for target thickness.

5.2. Effect of target strength or hardness on the ballistic performance

There are limited experimental data to show the affect of material strength on the ballistic performance of a small thickness target (or plate). Sangoy *et al.* [23] demonstrated that there are three zones in the hardness-ballistic limit relationships, i.e., (1) low hardness regime, where perforation resistance increases with hardness, (2) medium hardness regime, where the ballistic limit decreases due to the onset of adiabatic shear damage, and (3) high hardness regime, where perforation resistance increases again due to the projectile break-up. It means that ASB distinctly influences the ballistic performance. In an engineering perspective, it is usually assumed that the hardness is proportional to the material yielding strength; and thus, the monotonic relationship between the ballistic limit and target thickness and strength never come into existence. Instead it converts into an approximate relationship [23, 24], i.e., the variation of the ballistic limit may have a phenomenon of an "up-down-up" trend with an increase in the target thickness and strength.

Dey *et al.* [3] conducted a large amount of perforation tests on the steel alloy plates of Weldox 460E, Weldox 700E, and Weldox 900E respectively with thickness $H = 12$ mm, and analyzed the effect of target strength or hardness on the ballistic performance. The main discrepancy of the three steel alloys is that they have different yielding strength, i.e., 499 MPa, 859 MPa, and 992 MPa respectively. Thus, in this analysis we assume that the other parameters of Weldox 700E and Weldox 900E are same as those of Weldox 460E.

A Johnson-Cook material model is employed in Chen *et al.* [1] to discuss the influence of adiabatic shear failure, and the effect of target material strength is demonstrated as well. Figure 3 shows the critical velocity at initiation of adiabatic shear failure and the variation of the ballistic limit against the target material yielding a strength as predicted by Chen and Li [12], as well as the experimental results of ballistic limit. According to the model of shear plugging, the theoretical ballistic limit V_{BL} increases monotonously with the yielding stress (hardness) of plate material. On the other hand, according to the model of adiabatic shear plugging, the critical velocity V_A at adiabatic shear failure increases more gently with the yielding stress in the lower range of σ_y, and then gently

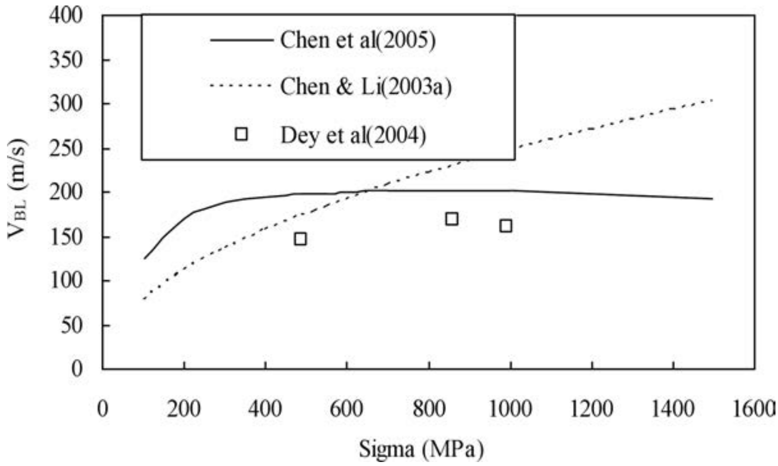

Fig. 3. Affect of plate strength on ballistic performance for $\chi = H/d = 0.6$.

decreases. Particularly in thinner plates, this phenomenon of up-and-down trend against σ_y seems more remarkable. It concludes that Chen *et al.* [1] may also have predicted the first two zones defined by Sangoy *et al.* [23]. In the present study, the projectile is assumed non-deformable, and thus, Fig. 3 demonstrates the performance in the low- to medium-hardness regime only, but fails to predict the phenomenon in the high-hardness regime.

Figures 4–6 show the test data of residual velocity of Weldox 460E, Weldox 700E, and Weldox 900E plates and the corresponding theoretical predictions by

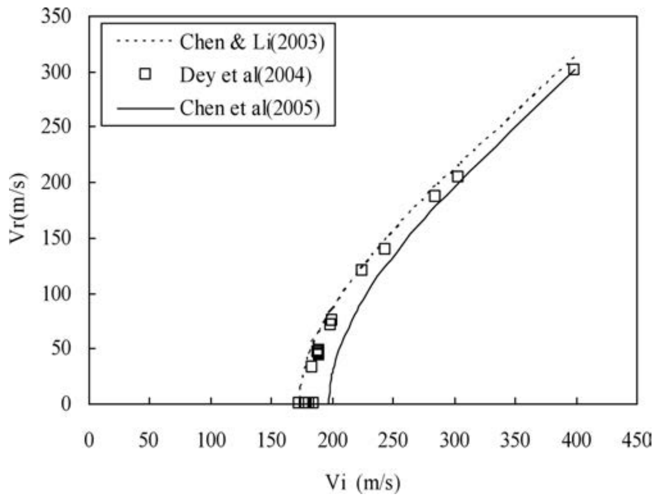

Fig. 4. Prediction of residual velocity and test data (Weldox 460E).

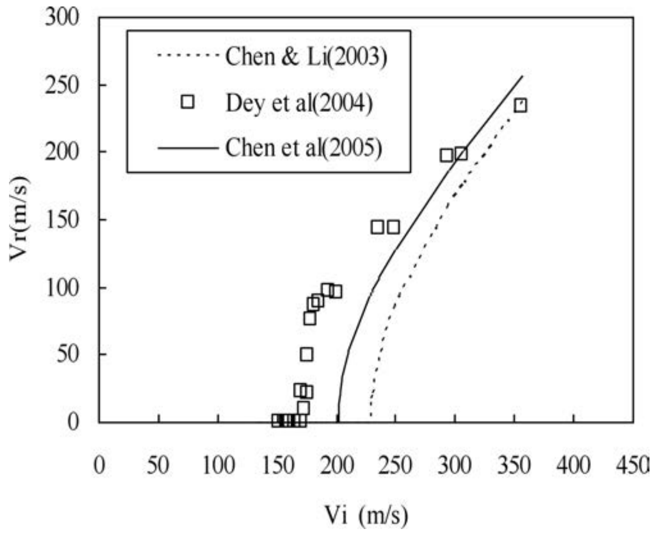

Fig. 5. Prediction of residual velocity and test data (Weldox 700E).

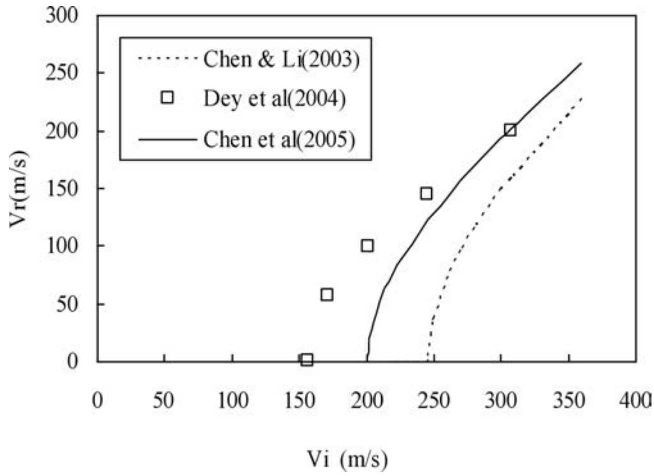

Fig. 6. Prediction of residual velocity and test data (Weldox 900E).

Chen and Li [12] and Chen *et al.* [1]. Obviously, for Weldox 460E, the test data of a lower impact velocity fits Chen and Li [12] well and implies that the dominating failure mode of the plate is shear plugging; whilst the data of a higher impact velocity locate between two models and thus shear plugging and adiabatic shear plugging both play an important role in plate perforation. Regarding Weldox 700E and Weldox 900E, all of the test data are close to Chen *et al.* [1] and the dominating failure mode of plate is adiabatic shear plugging.

The similar transition of perforation mode is also found in the sharp projectile striking Weldox 460E, Weldox 700E, and Weldox 900E plates [3]. In general, accompanied by an increase of target strength and thickness, the assumption of a rigid projectile trends to violated, and the perforation model tends toward transformation. It should be emphasized that any theoretical model has its specific applicable range.

6. Conclusions

Based on the analytical models by Chen and Li [12] and Chen *et al.* [1], the present paper analyzes the possible modes of shear plugging and adiabatic shear plugging in the perforation of metal plates struck by a blunt rigid projectile. The modified ballistic limit and residual velocity under the condition of adiabatic shear plugging are further formulated. Further experimental analyses were conducted on the perforations of Weldox E steel plates [2, 3], to discuss the affect of plate thickness and material strength/hardness on the terminal ballistic performance. More experimental evidence confirms the jump of residual velocity at ballistic limit induced by the structural response of plate. With increasing plate thickness and material strength, failure modes of plate may transform from shear plugging to adiabatic shear plugging. Due to adiabatic shear plugging, the monotonic relationship between the ballistic limit and target thickness and strength never come into existence.

References

1. Chen X.W., Li Q.M., Fan S.C., *Initiation of adiabatic shear failure in a clamped circular plate struck by a blunt projectile*, Int. J. Impact Eng., **31**, 7, 877–893, 2005.
2. Børvik T., Hopperstad O.S., Langseth M., Malo K.A., *Effect of target thickness in blunt projectile penetration of Weldox 460E steel plates*, Int. J. Impact Eng., **28**, 4, 413–464, 2003.
3. Dey S., Børvik T., Hopperstad O.S., Leinum J.R., Langseth M., *The effect of target strength on the perforation of steel plates using three different projectile nose shapes*, Int. J. Impact Eng., **30**, 1005–1038, 2004.
4. Backman M.E., Goldsmith W., *Mechanics of penetration of projectiles into targets*, Int. J. Impact Eng., **16**, 1–99, 1978.
5. Anderson Jr. C.E., Bodner S.R., *Ballistic impact: the status of analytical and numerical modeling*, Int. J. Impact Eng., **7**, 9–35, 1988.
6. Corbett G.G., Reid S.R., Johnson W., *Impact loading of plates and shells by free-flying projectiles: a review*, Int. J. Impact Eng., **18**, 141–230, 1996.
7. BenDor G., Dubinsky A., Elperin T., *Ballistic impact: recent advances in analytical modeling of plate penetration dynamics-a review*, ASME Applied Mechanics Reviews, **58**, 11, 355–371, 2005.
8. Børvik T., Langseth M., Hopperstad O.S., Malo K.A., *Ballistic penetration of steel plates*, Int. J. Impact Eng., **22**, 855–886, 1999.
9. Børvik T., Leinum J.R., Solberg J.K., Hopperstad O.S., Langseth M., *Observations on shear plug formation in Weldox 460E steel plates impacted by blunt-nosed projectiles*, Int. J. Impact Eng., **25**, 553–572, 2001.
10. Børvik T., Langseth M., Hopperstad O.S., Malo K.A., *Perforation of 12 mm thick steel plates by 20 mm diameter projectiles with blunt, hemispherical and conical noses, Part I: Experimental study*, Int. J. Impact Eng., **27**, 1, 19–35, 2002.
11. Børvik T., Hopperstad O.S., Berstad T., Langseth M., *Perforation of 12 mm thick steel plates by 20 mm diameter projectiles with blunt, hemispherical and conical noses, Part II: Numerical simulations*, Int. J. Impact Eng., **27**, 1, 37–64, 2002.
12. Chen X.W., Li Q.M., *Shear plugging and perforation of ductile circular plates struck by a blunt projectile*, Int. J. Impact Eng., **28**, 5, 513–536, 2003.
13. Chen X.W., Li Q.M., *Perforation of a thick plate by rigid projectiles*, Int. J. Impact Eng., **28**, 7, 743–759, 2003.
14. Chen X.W., Li Q.M., Fan S.C., *Oblique perforation of thick metallic plates by rigid projectiles*, ACTA Mechanic Sinica, **22**, 367–376, 2006.

15. Chen X.W., Yang Y.B., Lu Z.H., Chen Y.Z., *Perforation of Metallic Plates Struck by a Blunt Projectile with a Soft Nose*, Int. J. Impact. Eng., **35**, 6, 549–558, 2008.

16. Chen X.W., Zhou X.Q., Li X.L., *On Perforation of Ductile Metallic Plates by Blunt Rigid Projectile*, European Mechanics/A, **28**, 2, 273–283, 2009.

17. Wen H.M., Jones N., *Low-velocity perforation of punch-impact-loaded metal plates*, J. Pressure Vessel Technol., **118**, 2, 181–7, 1996.

18. Bai Y.L., Johnson W., *Plugging: physical understanding and energy absorption*, Metals Technol., **9**, 182–90, 1982.

19. Ravid M., Bodner S.R., *Dynamic perforation of viscoplastic plates by rigid projectiles*, Int. J. Impact Eng., **21**, 6, 577–91, 1983.

20. Recht R.F., Ipson T.W., *Ballistic perforation dynamics*, J. Appl. Mech., **30**, 385–91, 1963.

21. Srivathsa B., Ramakrishnan N., *On the Ballistic Performance of Metallic Materials*, Bull. Mater. Sci., **20**, 1, 111–23, 1997.

22. Srivathsa B., Ramakrishnan N., *A ballistic performance index for thick metallic armour*, Comput. Model Simul. Eng., **3**, 1, 33–39, 1998.

23. Sangoy L., Meunier Y., Pont G., *Steels for ballistic protection*, Israel J. Tech., **24**, 319–26, 1988.

24. Li Q.M., Chen X.W., *Penetration and Perforation into Metallic Targets by a Non-deformable Projectile*, Chapter 10, pp. 173–192, Engineering Plasticity and Impact Dynamics (Edt. Zhang LZ), World Scientific Publishing, 2001.

25. Bai Y.L., Dodd B., *Adiabatic shear localization: occurrence, theories and application*, UK: Pergamon Press, 1992.

Received January 11, 2011; revised version August 2, 2011.